LUMINESCENCE AND SPECTRAL CHARACTERISTICS OF ZINC SULFIDE NANOPARTICLES DOPED WITH Eu^{2+}

A. V. Selishchev and V. V. Pavlishchuk

UDC 546.47.222.1,546.661,535.372,544.174.2

A method is proposed for the production of zinc sulfide nanoparticles with an average size of 6.0 ± 1.0 nm, doped with Eu^{2+} ions (molar ratio Eu : Zn ≈ 0.01%-0.19%), by simultaneous decomposition of diethyldithiocarbamate complexes of zinc(II) and europium(II) in high-boiling solvents. It was established that the position of the emission band at 645 nm for the obtained $ZnS : Eu^{2+}$ nanoparticles hardly depends at all on the europium content while the luminescence intensity is highest with a dopant content of 0.05%. It was shown that the emission band for the $ZnS : Eu^{2+}$ nanoparticles arises from Eu^{2+} emission centers localized on the surface of the nanoparticles.

***Key words**: zinc sulfide, doping, europium, luminescence, surface, monomolecular precursors.*

One method of giving broad-band semiconductors and dielectrics the ability to luminesce and improving their luminescence characteristics is to dope them with the ions of $3d$ and $4f$ metals [1]. Such bulk and film-type materials based on oxides, sulfides, silicates, phosphates, vanadates, and other types of compounds have already found use in luminescent screens, lighting fixtures, optical sensors, and lasers [2]. At the same time in connection with the need to miniaturize optoelectronic devises and develop medical sensors for work at the cellular level it is today appropriate to create nanosized luminescent items (nanoparticles, nanorods, nanoplates, etc.) doped with the ions of $3d$ and $4f$ metals and also to study their spectral characteristics [3].

In this connection zinc sulfide nanoparticles, which meet the main requirements for phosphor crystals (optical transparency in the visible part of the spectrum and high chemical stability), are of considerable interest as subjects for doping [4]. At the same time individual zinc sulfide has low-intensity luminescence in the shortwave part of the visible spectrum, due to recombination with the participation of defects, and to improve the luminescence characteristics it must be activated by ions having their own emitting transitions, on the one hand, and capable of being embedded in its crystal lattice, on the other [1, 2]. Thus, doping of ZnS nanoparticles with the ions of the $3d$ metals Cu^{2+} and Mn^{2+} with ionic radii, coordination numbers, and formal charges close to those of Zn^{2+} leads to the appearance of bright "green" and "orange" luminescence respectively. The emission in such luminophores occurs as a result of d–d transitions in the ions of the dopants, the prohibition on which is partly removed on account of the splitting of the corresponding terms by the crystal field that is promoted by incorporation of these ions in the ZnS lattice [4, 5]. In the case of the doping of ZnS with Ln^{3+} ions, the radii of which are substantially larger than the radius of Zn^{2+} and which have larger coordination numbers, only low-intensity luminescence is observed if the co-dopants are not added [5]. This is explained both by the difficulty of inserting the Ln^{3+} ions into the ZnS lattice and by the small extinction coefficients of the corresponding forbidden f–f transitions for the Ln^{3+} ions. This problem can be resolved partly by using Eu^{2+}

ions, which have strong permitted $4f$–$5d$ transitions. Although they differ from Zn^{2+} ions in ionic radius ($r_{Zn^{2+}} = 0.74$ Å, $r_{Eu^{2+}} = 1.09$ Å [6]) Eu^{2+} ions do, however, have the same formal charge of 2+, which facilitates their entry into the ZnS lattice and according to [7-12] gives the ZnS ions doped with Eu^{2+} ($ZnS : Eu^{2+}$) the ability to emit light in the visible region.

Earlier it was shown that luminescence with maxima at 670 and 580 nm is observed for $ZnS : Eu^{2+}$ with sizes of 4.2 and 3.2 nm respectively. By analogy with the emission of bulk $ZnS : Eu^{2+}$ ($\lambda_{max} = 695$ nm [7]) this was explained by the recombination of excitons associated with the Eu^{2+} [8]. The $ZnS : Eu^{2+}$ nanoparticles with diameter of 2.6 nm were characterized by emission of light with a maximum at 520 nm, which in the opinion of the authors of [9] was caused by the $4f$–$5d$ transition in the Eu^{2+} ion made possible by enlargement of the forbidden band of the ZnS nanoparticles under the conditions of spatial restriction of the exciton. At the same time emission of light in a similar range ($\lambda_{max} = 520$ nm) was observed for $ZnS : Eu^{2+}$ nanoparticles not affected by the quantum-size effect [10]. The emission of light by comparatively large $ZnS : Eu^{2+}$ nanoparticles with sizes of 28 and 50 nm with emission maxima at 480 and 475 nm respectively was also reported [11, 12]. Thus, existing data on the spectral region of luminescence in $ZnS : Eu^{2+}$ nanostructures are contradictory in nature, and it is clear that the position of the luminescence band of nanosized ZnS doped with Eu^{2+} ions is also determined by other factors in addition to the size of the nanoparticles.

In our opinion one of the possible reasons for the discrepancies in the luminescence characteristics of $ZnS : Eu^{2+}$ presented in the literature may be the presence in the $ZnS : Eu^{2+}$ nanoparticles of halogen-containing or oxygen-containing co-dopant impurities, which on account of high affinity to the hard ions of the lanthanides coordinate with the Eu^{2+} and have a significant effect on the position of the emission band. Another possible reason for the change of the spectral region of emission may lie in localization of the Eu^{2+} ions in the volume or on the surface of the nanostructures, which may be a significant factor as a result of the large proportion of surface atoms in the nano subjects. In all probability the nature of the closest environment of the Eu^{2+} ions is determined by the conditions under which the $ZnS : Eu^{2+}$ nanoparticles are synthesized. Earlier it was shown that the production of individual nanoparticles of europium(II) sulfide EuS and zinc sulfide ZnS can be achieved in particular by thermal decomposition of the monomolecular precursors [13, 14]. It is extremely likely that the joint decomposition of a mixture of monomolecular sulfur-containing precursors of the two metals, which the dithiocarbmates are, can lead to entry of the Eu^{2+} ions into the ZnS lattice in the closest environment of the sulfide ions without the co-dopants of chloride, nitrate, and other anions as impurities. By the method of decomposition of monomolecular precursors it is also possible to synthesize structures of the core–shell type [15], and it can be supposed that successive decomposition of zinc(II) and europium(III) complexes will lead to the formation of nanoparticles of zinc sulfide with Eu^{2+} ions immobilized on their surface. By subsequent creation of a shell of zinc sulfide on such nanoparticles it may be possible to study the possible participation of surface Eu^{2+} ions in the luminescence processes. The aim of the present work was to produce ZnS nanoparticles doped with Eu^{2+} by decomposition of monomolecular dithiocarbamate complexes of zinc(II) and europium(III) and to study the effect of localization of europium in the volume and on the surface of the ZnS nanoparticles doped with Eu^{2+} on their spectral characteristics.

EXPERIMENTAL

The commercially available reagents $Zn(NO_3)_2 \cdot 6H_2O$ and $Eu(NO_3)_3 \cdot 6H_2O$ were used without further purification. Before use the high-boiling solvents oleylamine (OA) and 1-octadecene (ODE) were degassed, dehydrated at 90-100 °C under vacuum, and placed in an atmosphere of argon. Europium(III) diethylammonium tetrakis(N,N-diethyldithiocarbamate) ($NH_2Et_2[Eu(Ddtc)_4]$) and sodium diethyldithiocarbamate were synthesized according to the procedures in [13, 16].

Zinc(II) bis(N,N-diethyldithiocarbamate) ($Zn(Ddtc)_2$) was obtained by precipitation from aqueous solutions of zinc nitrate and sodium diethyldithiocarbamate. It was recrystallized from chloroform and dried to constant weight over P_2O_5. Found, %: C 33.20; H 5.56; N 8.06. Calculated, %: C 34.09; H 5.68; N 7.95.

Synthesis of $ZnS : Eu^{2+}$ Nanoparticles by Joint Decomposition of Complexes. 400 mg (1.11 mmol) of $Zn(Ddtc)_2$ was dissolved in a mixture of 10 mL (29.4 mmol) of OA and 14 mL (70 mmol) of ODE. The solution was degassed at 60-70 °C after which it was blown with argon. In order vary the Eu^{2+} content of the zinc sulfide nanoparticles the necessary amount of a 0.02 M solution of $NH_2Et_2[Eu(Ddtc)_4]$ in OA was added to the obtained transparent solution under argon with agitation for 30 min. Simultaneous decomposition of the initial reagents was achieved by gradually heating the reaction mixture to 240 °C

and then holding it at this temperature for 1 h. The excess of the high-boiling solvents was removed by dispersing the nanoparticles in chloroform, precipitating them with methanol, and separating them by centrifuging. The purification procedure was repeated three times.

Synthesis of ZnS@Eu²⁺ Nanoparticles by Successive Decomposition of the Complexes. We placed 400 mg (1.11 mmol) of $Zn(Ddtc)_2$, 10 mL (29.4 mmol) of OA, and 14 mL (70 mmol) of ODE in the reaction vessel. The mixture was degassed by heating under vacuum, filled with argon, heated to 240 °C, and kept for 1 h as described above. A 0.28- mL portion (0.0056 mmol) of a 0.02 M solution of $NH_2Et_2[Eu(Ddtc)_4]$ in OA was then added drop by drop to the reaction mixture at the same temperature, and the mixture was kept for a further 1 h. The product was purified by dispersing three time in chloroform and precipitation with methanol.

Synthesis of ZnS@Eu²⁺@ZnS with the Formation of a ZnS Shell. First, in accordance with the previous procedure, a fresh dispersion of the ZnS@Eu²⁺ sample in OA/ODE was obtained by successive decomposition of the $Zn(Ddtc)_2$ and $NH_2Et_2[Eu(Ddtc)_4]$ complexes. Then, without isolating the precipitate and still keeping the temperature at 240 °C in order to form a ZnS shell, we added a solution of 400 mg of $Zn(Ddtc)_2$ in 3 mL of OA drop by drop over 15 min and kept the mixture at 240 °C for 45 min. The product was purified as described above.

The powder diffractograms were obtained on a Bruker D8 Advance diffractometer (CuK_α, $\lambda = 1.5406$ Å). The instrumental broadening was determined with crystalline silicon as standard. Photomicrographs were obtained on a Selmi PÉM-125K transmission electron microscope at an accelerating voltage of 100 kV. The average sizes of the nanoparticles were determined by statistical analysis of the sizes of more than 200 individual objects. The electronic spectra of the dispersions and solutions were recorded on a Specord 200 spectrophotometer, while the diffuse reflection spectra were recorded on a Carl Zeiss (Jena) Specord M-40 spectrophotometer. The luminescence spectra were measured on a Perkin Elmer LS 55 spectrometer at room temperature and were reduced to identical absorption at the wavelength of the exciting radiation $\lambda = 335$ nm. The carbon, nitrogen, and hydrogen contents were determined on a Carlo Erba 1106 CHN analyzer. The Zn/Eu molar ratio was determined on an ElvaX SER-01 X-ray fluorescence analyzer with a W anode. The ESR spectra were recorded on an Adani CMS 8400 spectrometer in the X range. The sizes of the ZnS nanoparticles in the dispersions were established by dynamic light scattering (DLS) on a Malvern ZetaSizer Nano-S analyzer (ZEN 1600) using a refractive index of 2.35 [14].

RESULTS AND DISCUSSION

The phase composition of the obtained nanoparticles was established by X-ray (XRD) and electron-diffraction (ED) analysis (Fig. 1a-e). All the X-ray reflections and electron-diffraction data of the obtained samples are characteristic of the sphalerite modification of ZnS. The unit cell parameter a, calculated from the X-ray and electron data, amounted to 5.42 ± 0.02 and 5.39 ± 0.05 Å, which corresponds within the experimental error limits to the unit cell parameter a characteristic of bulk cubic ZnS, 5.41 Å [14]. On the electron-diffraction patterns of the samples there were solid ring-shaped reflections, indicating in favor of the formation of small-sized nanoparticles. The presence of europium in the samples was confirmed by the data from X-ray fluorescence spectroscopy. Here the europium content in the obtained ZnS : Eu²⁺ was substantially lower than the amount added to the reaction mixture (Table 1), which may be due to the above-mentioned difficulties for entry of the Eu²⁺ into the crystal lattice of the ZnS as a result of differences in the ionic radii of Zn^{2+} and Eu^{2+} and also the different coordination numbers characteristic of these ions. The presence of europium(II) in the samples was also confirmed by the presence of a signal with a g factor of 2.000 ± 0.001 in the ESR spectra (Fig. 1f) and by the hyperfine structure, which may correspond to splitting at the Eu²⁺ nuclei (nuclear spin $I = 5/2$) [12] and moreover by the fact that Eu³⁺ is not detected under the experimental conditions by ESR on account of the zero resultant spin magnetic moment of the ground state $^7F_0$ of the $4f^6$ configuration [17]. As follows from the TEM data (Fig. 1a-d), the form of the obtained nanoparticles is close to spherical. The average sizes of the nanoparticles determined by the TEM method, by dynamic light scattering, and from the X-ray diffraction data using Scherrer equation proved almost identical within the experimental limits for the ZnS : Eu²⁺ samples with various dopant contents (Table 1). Thus, it is possible by the proposed method to produce ZnS : Eu²⁺ nanoparticles with average sizes of 6.0 ± 1.0 nm differing in europium(II) content.

In order to monitor the formation of ZnS : Eu²⁺ nanoparticles from the reaction mixture containing the initial zinc(II) and europium(III) complexes in oleylamine and 1-octadecene as medium we took aliquot portions at specific temperatures and
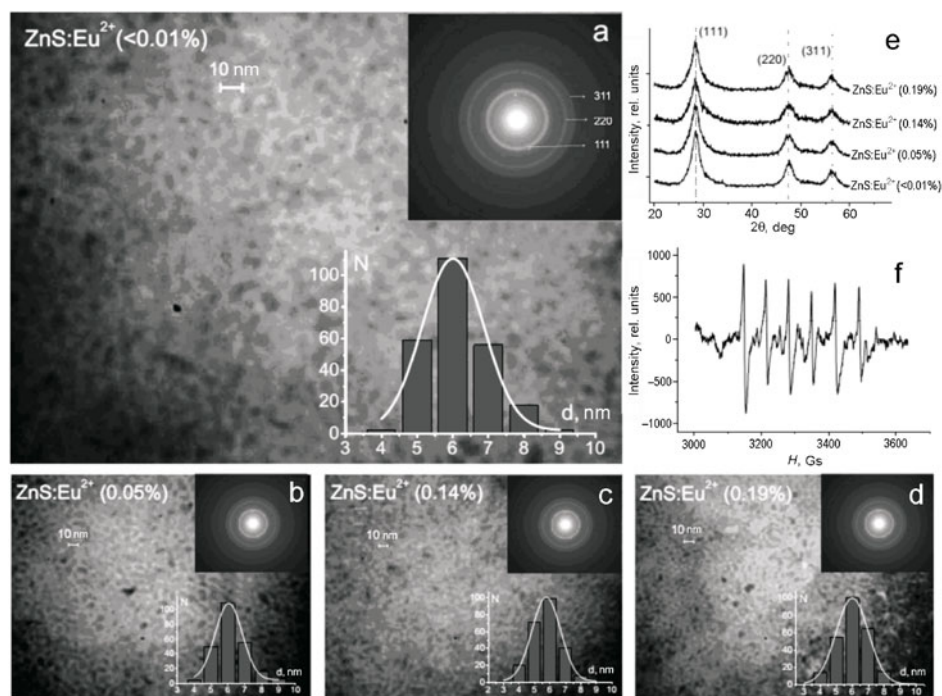
Fig. 1. Photomicrographs (a-d) (top inset, electron diffraction patterns; bottom inset, size distribution of particles) and X-ray diffraction (e) of ZnS : Eu^{2+} nanoparticles with various europium contents and the ESR spectrum of the ZnS : Eu^{2+} nanoparticles (0.14%) (f).

TABLE 1. Characteristics of ZnS and ZnS : Eu^{2+} Nanoparticles

Nanoparticles	Eu : Zn Molar ratio, %		Average size of particles d, nm		
	added to reaction mixture	determined experimentally	TEM	DLS	XRD
ZnS : Eu^{2+}	2.5	0.19 ± 0.01	6.0 ± 1.0	7.6 ± 2.4	4.6 ± 1.0
ZnS : Eu^{2+}	1.0	0.14 ± 0.01	5.8 ± 0.9	7.9 ± 2.0	4.2 ± 1.0
ZnS : Eu^{2+}	0.5	0.05 ± 0.01	6.0 ± 0.8	7.9 ± 1.8	4.2 ± 1.0
ZnS : Eu^{2+}	0.1	<0.01	6.0 ± 0.9	7.0 ± 2.1	4.6 ± 1.0
ZnS	0	0	6.2 ± 1.3	7.0 ± 1.9	–
ZnS@Eu^{2+}	0.5	0.04 ± 0.01	6.2 ± 1.1	7.4 ± 1.6	4.5 ± 1.0
ZnS@Eu^{2+}@ZnS	0.25	0.02 ± 0.01	7.7 ± 1.0	9.7 ± 1.9	5.8 ± 1.0

fixed time intervals. After dilution with chloroform the electronic spectra were measured, and the sizes of the nanoparticles were determined by dynamic light scattering. Beginning at 150 °C the absorption bands of the initial zinc dithiocarbamate with maxima at 260 and 280 nm belonging to intraligand π–π* transitions disappeared (Fig. 2a), indicating decomposition of the complex. Here, a new band with absorption edge at ~316 nm, belonging in all probability to absorption of light by nanoparticles of the semiconductor ZnS [14], appeared. However, the indicated temperature 150 °C is insufficient for the formation of europium(II) sulfide from NH$_2$Et$_2$[Eu(Ddtc)$_4$] [15, 18]. Further heating of the reaction medium to 240 °C, at which reduction of
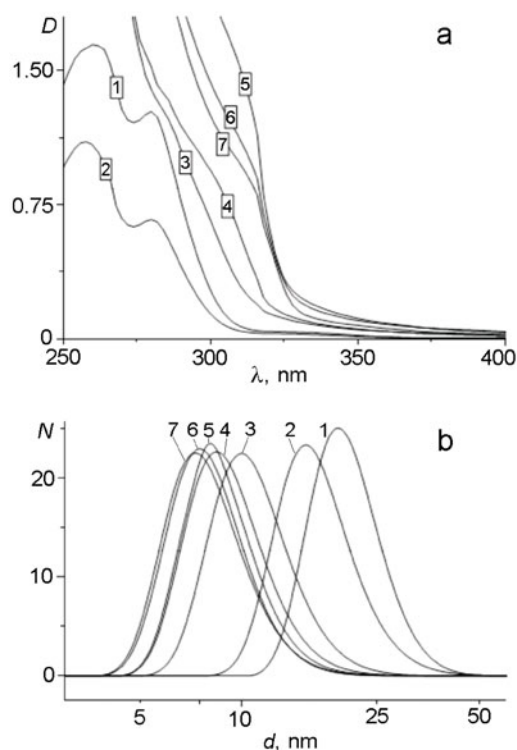
Fig. 2. Dynamics of change of electronic spectra (a) and sizes of nanoparticles according to DLS data (b) in the formation and growth of ZnS : Eu^{2+} nanoparticles (0.14%): 1) 50 °C; 2) 100 °C; 3) 150 °C; 4) 200 °C; 5) 240 °C; 6) 240 °C, 5 min; 7) 240 °C, 60 min.

Eu^{3+} to Eu^{2+} under the reaction conditions has already become possible, was accompanied by a bathochromic shift of the edge of the absorption band of ZnS, which may indicate an increase in the size of the nanoparticles. Holding the reaction mixture at 240 °C for 1 h did not lead to a significant change in the position of the edge of the absorption band of ZnS ($\lambda \approx 330$ nm). The absence of a band corresponding to the absorption of the Eu^{2+} ions in the electronic spectra recorded for the aliquots may result from its low intensity on account of the small content of Eu^{2+} in the samples (Table 1). It is interesting to note that the dynamics of variation of the electronic spectra corresponds exactly to the changes of the particle sizes in the dispersions. According to the DLS data (Fig. 2b) the initial complex Zn(Ddtc)$_2$ in a mixture of OA and ODE exists in the form of aggregates with an average size of 20-25 nm. On heating in the range of 150-240 °C the average sizes, in all probability, of the mixture of aggregates and non-aggregated nanoparticles in the dispersion were greatly reduced (Fig. 2b), and 5 min after heating to 240 °C they already remained practically unchanged. This can be interpreted as the end of decomposition of the complex and the formation of ZnS : Eu^{2+} nanoparticles with the final sizes (Table 1). Thus, when the temperature of the reaction mixture has reached 240 °C the ZnS nanoparticles have already completed their growth and the formation of Eu^{2+} ions is only beginning, from which it can be supposed that the Eu^{2+} ions in the obtained ZnS : Eu^{2+} samples are localized not in the volume of the ZnS nanoparticles but close to their surface.

In the electronic spectra of the final-sized ZnS : Eu^{2+} nanoparticles recorded for the dispersions in chloroform, for all the samples obtained the absorption band with the edge of ~330 nm (Fig. 3a) was observed, corresponding to the absorption of light by ZnS semiconductor. The value of E_g calculated by the Tauc method in $(Dh\nu)^{1/n}$–$h\nu$ coordinates with an exponent $n = 1/2$ for direct allowed transitions was 3.85 ± 0.01 eV. The resulting value of the band gap of the semiconductor is slightly higher than the value of $E_g \approx 3.6$ eV for the bulk ZnS of sphalerite modification [5, 14, 19], which may be the result of manifestation of the quantum size effect in the weak spatial confinement of the exciton [20]. The band, corresponding to absorption by Eu^{2+} ions, for
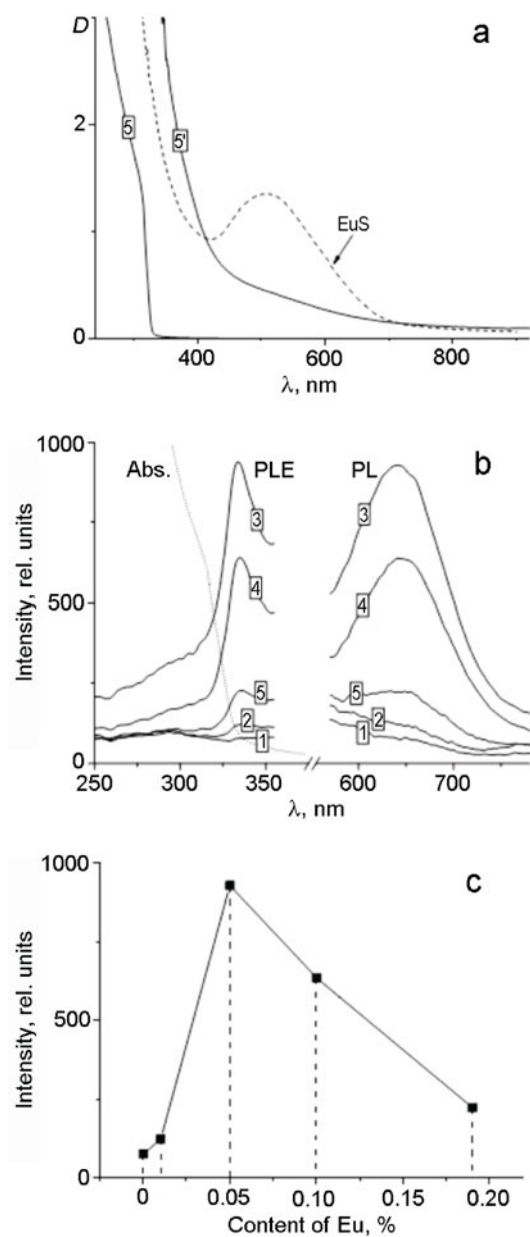
Fig. 3. a) Electronic absorption spectra in chloroform of ZnS : Eu^{2+} (0.19%) nanoparticles in dilute (5) and concentrated (5′) dispersions (the electronic spectrum of EuS nanoparticles is reprinted from [18]). b) Photoluminescence (PL), and photoluminescence excitation (PLE) spectra of ZnS (1) and ZnS : Eu^{2+} nanoparticles with europium contents of <0.01% (2), 0.05% (3), 0.14% (4), and 0.19% (5) and the electronic absorption (abs.) spectrum of ZnS : Eu^{2+} nanoparticles (0.14%). c) Dependence of the luminescence intensity of ZnS : Eu^{2+} nanoparticles on the europium content.

dilute dispersions of ZnS : Eu^{2+} nanoparticles was not detected (Fig. 3a), presumably as described above, due to the low content of europium in the samples. Meanwhile, in the electronic spectra recorded for the concentrated nanoparticle dispersions of

ZnS : Eu^{2+}, on the background of a significant light scattering a shoulder was observed in the range of 400-700 nm, which by analogy with absorption of EuS ($\lambda_{max} \approx 505$ nm [18]) can be referred to absorption associated with Eu^{2+} ions (Fig. 3a).

In the luminescence spectra of the ZnS : Eu^{2+} nanoparticles, measured for the dry powders at room temperature, there was a broad emission band with a maximum at 645 nm (Fig. 3b) the intensity of which depended on the concentration of Eu^{2+}. In the luminescence excitation spectrum there was a band with $\lambda_{max} \approx 335$ nm, corresponding to the edge of the absorption band of ZnS in the electronic spectra (Fig. 3a,b). This may indicate an indirect mechanism of excitation of luminescence by transfer of energy absorbed by the nanoparticles of the ZnS semiconductor to the luminescence levels of the ZnS : Eu^{2+} composite. The slight shift of the maximum of the excitation band in relation to the absorption band of ZnS is typical of the transfer of energy from the phosphor crystal base to the emissive impurity centers [5]. The nature of the appearance of the emission band observed for the ZnS : Eu^{2+} nanoparticles, by analogy with the assignment of the emission bands of Eu^{2+} in the CaS and SrS sulfide matrices [15], may result from intraionic electron transfer of Eu^{2+} from the excited $4f^65d^1$ state to the ground state $4f^7$ ($^8S_{7/2}$). A further argument in favor of this proposal may be provided by the proximity of the spectral regions in which the given emission band is observed ($\lambda_{max} \approx 660$ nm for CaS : Eu^{2+} and $\lambda_{max} \approx 610$ nm for SrS : Eu^{2+}). The absence of the band corresponding to the $4f^7$–$4f^65d^1$ transition of Eu^{2+} in the luminescence excitation spectra, like its absence in the absorption spectra, may result from the small ~0.01%-0.19% content of Eu^{2+} in the samples. An alternative explanation for the nature of the appearance of luminescence in ZnS doped with Eu^{2+} [7, 21] presupposes degeneracy in the $5d$ orbitals of Eu^{2+} in the conduction band of ZnS, where the emission of light is caused by recombination of excitons associated with Eu^{2+}. The holes of such excitons are thought to be localized at the $4f^6$ orbitals of the Eu^{3+} ions, formed as a result of the occurrence of Eu$^{2+} \rightarrow$ Eu$^{3+} + e$ ionization processes, while the relaxing electrons occupy sublevels located somewhat lower than the bottom of the conduction band of the ZnS semiconductor. Thus, the ground state of the emissive transition observed for ZnS : Eu^{2+} is in all probability the localized levels of the $4f^6$ configuration of europium. At the same time a reliable explanation for the nature of the excited state under discussion as a result of the proximity of the $5d$ orbitals of Eu^{2+} to the conduction band of ZnS is not possible on the basis of existing data and may provide a subject for future investigations.

A series of samples with various contents of europium in relation to zinc were prepared in order to investigate the possible connection between the intensity of the observed emission and the concentration of europium (see Table 1). Luminescence in the investigated region was not observed for the sample of ZnS not containing europium, but a constant emission band with a maximum at 645 nm was observed for the samples containing europium. The dependence of the luminescence intensity on the europium concentration passed through a maximum (Fig. 3c), indicating concentration quenching of the luminescence. It is interesting to note that the observed effect makes it possible to explain the absence of luminescence due to Eu^{2+} for the nanoparticles of individual europium sulfide EuS by concentration quenching of light emission by Eu^{2+} ions.

In order to study the effect of the position of the Eu^{2+} ions on the spectral characteristics of ZnS nanoparticles doped with Eu^{2+} samples of ZnS@Eu^{2+} and ZnS@Eu^{2+}@ZnS, in which the europium is assumed to be immobilized on the surface and incorporated in the volume of the ZnS respectively, were produced by successive decomposition of the initial complexes. During production of the sample of ZnS@Eu^{2+} nanoparticles of the individual ZnS were first synthesized, and the NH$_2$Et$_2$[Eu(Ddtc)$_4$] complex was then added to their dispersion in high-boiling solvents and thermally decomposed. The presence of europium in the sample was confirmed by the data from X-ray fluorescence analysis. Since the sizes of the ZnS@Eu^{2+} nanoparticles in relation to the sizes of the individual ZnS nanoparticles did not change (Table 1) this may indicate that the Eu^{2+} ions are immobilized on the surface of the nanoparticles. During the production of the ZnS@Eu^{2+}@ZnS sample a shell of zinc sulfide was formed around the ZnS@Eu^{2+} nanoparticles by decomposition of another portion of the Zn(Ddtc)$_2$ complex. The formation of the shell is confirmed by the increase of the average sizes of the nanoparticles from 6.2 ± 1.1 nm for the ZnS@Eu^{2+} sample to 7.7 ± 1.0 nm for the ZnS@Eu^{2+}@ZnS sample (Fig. 4a,b). According to the data from X-ray fluorescence analysis the Eu/Zn molar ratio in the ZnS@Eu^{2+}@ZnS sample decreased in inverse proportion to the total amount of zinc used on the formation of the core and shell of the ZnS. This corresponds to quantitative, within the error limits of the determination method, transition of europium from ZnS@Eu^{2+} to ZnS@Eu^{2+}@ZnS and indicates that the Eu^{2+} is located in the volume of the ZnS@Eu^{2+}@ZnS nanoparticles (Table 1). In the luminescence spectrum, recorded for the dry ZnS@Eu^{2+} powder, there was a band at 645 nm comparable in intensity with the analog ZnS : Eu^{2+} (Fig. 4c), from which it can be concluded that the luminescence of both ZnS : Eu^{2+} and ZnS@Eu^{2+} arises primarily from the surface emission centers linked
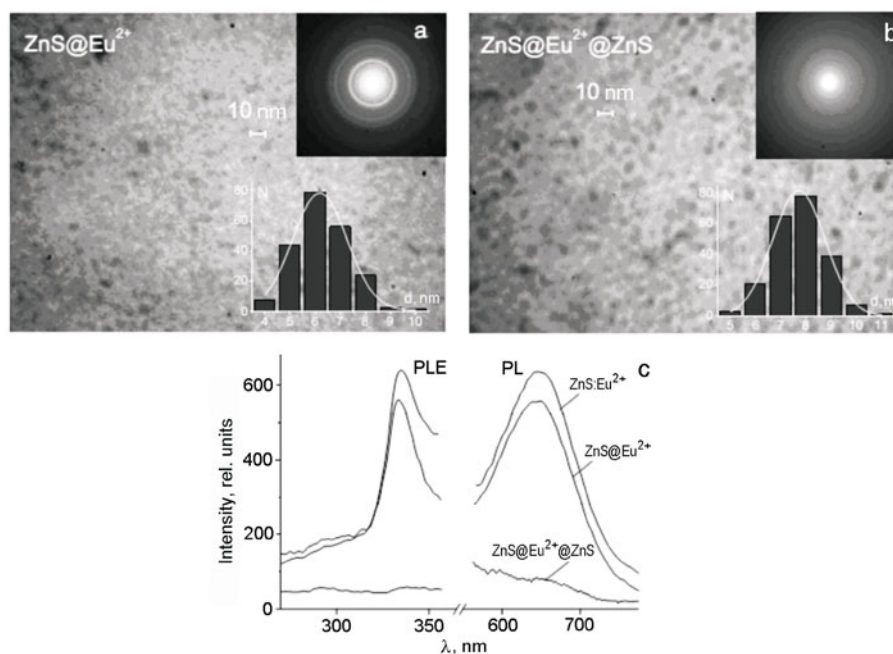
Fig. 4. Photomicrographs (a, b) of the $ZnS@Eu^{2+}$ and $ZnS@Eu^{2+}@ZnS$ nanoparticles (top inset, electron-diffraction patterns; bottom inset, size distribution of the particles) and the photoluminescence (PL) and photoluminescence excitation (PLE) spectra (c) of the $ZnS@Eu^{2+}$ and $ZnS@Eu^{2+}@ZnS$ nanoparticles in comparison with the analogous spectra of the $ZnS : Eu^{2+}$ nanoparticles (0.05%).

with the Eu^{2+}. Here, in the luminescence spectrum recorded for the dry $ZnS@Eu^{2+}@ZnS$ powder the analogous emission band has practically disappeared, which confirms that the luminescence appears as a result of the surface centers. It can be assumed that the presence of the Eu^{2+} in the volume of the zinc sulfide in the environment of the sulfide ions by analogy with bulk $ZnS : Eu^{2+}$ leads to degeneracy of the emission levels in the conduction band of the ZnS [7]. Here, the significant decrease of the intensity of the emission band for the $ZnS@Eu^{2+}@ZnS$ nanoparticles does not contradict the data on the luminescence of bulk $ZnS : Eu^{2+}$ in view of the fact that the intensity of the latter at room temperature was also insignificant [7].

Thus, the present work has shown that the simultaneous decomposition of zinc(II) and europium(III) diethyldithiocarbamate complexes leads to the formation of ZnS nanoparticles doped with Eu^{2+} having average sizes of 6.0 ± 1.0 nm. It was found that the dependence of the luminescence intensity of the $ZnS : Eu^{2+}$ nanoparticles at 645 nm on the europium content passes through a maximum, and the observed emission band is due to the presence of Eu^{2+} in the obtained samples. By immobilizing the europium on the surface of the ZnS and forming a shell of ZnS around such a composite it was shown that the observed emission band of the ZnS nanoparticles doped with Eu^{2+} is due to emission centers located on the surface of the nanoparticles.

REFERENCES

1. Y. Zhang and J. Hao, *J. Mater. Chem. C*, **1**, No. 36, 5607-5618 (2013).
2. G. Blasse and B. C. Grabmaier, *Luminescent Materials*, Springer Verlag, Berlin, Heidelberg (1994).
3. S. Sheng and Q. Wang, *Chem. Mater.*, **25**, No. 8, 1166-1178 (2013).
4. S. R. Rotman (ed.), *Wide-Gap Luminescent Materials: Theory and Applications*, Springer Science + Business Media, New York (1997).

5. H. Hu and W. Zhang, *Opt. Mater.*, **28**, No. 5, 536-550 (2006).

6. V. Shanker and H. Chander, *Handbook of Electroluminescent Materials*, IOP Publishing, Bristol (2004), Ch. 5, pp. 193-216.

7. K. Swiatek, M. Godlewski, and D. Hommel, *Phys. Rev. B*, **42**, No. 6, 3628-3633 (1990).

8. W. Chen, J. O. Malm, V. Zwiller, et al., *J. Appl. Phys.*, **89**, No. 5, 2671-2675 (2001).

9. W. Chen, J.-O. Malm, V. Zwiller, et al., *Phys. Rev. B*, **61**, No. 16, 11021-11024 (2000).

10. B. Cheng and Z. Wang, *Adv. Funct. Mater.*, **15**, No. 11, 1883-1890 (2005).

11. G. Sharma, S.-D. Han, S. P. Khatkar, et al., *ECS Trans.*, doi:10.1149/1.2209392 (2006).

12. M. Hossu, R. O. Schaeffer, and L. Ma, *Opt. Mater.*, **35**, No. 8, 1513-1519 (2013).

13. M. D. Regulacio, S. Kar, Ed. Zuniga, et al., *Chem. Mater.*, **20**, No. 10, 3368-3376 (2008).

14. D. C. Onwudiwe, C. Strydom, O. S. Oluwafemi, and S. P. Songca, *Mater. Res. Bull.*, **47**, No. 12, 4445-4451 (2012).

15. Y. Zhao, F. T. Rabouw, T. van Puffelen, et al., *J. Am. Chem. Soc.*, **136**, No. 47, 16533-16543 (2014).

16. V. M. Byr'ko, *Dithiocarbamates* [in Russian], Nauka, Moscow (1984).

17. H. Song, H. Yu, G. Pan, et al., *Chem. Mater.*, **20**, No. 14, 4762-4767 (2008).

18. A. V. Selishchev and V. V. Pavlishchuk, *Teor. Éksp. Khim.*, **50**, No. 1, 39-45 (2014). [*Theor. Exp. Chem.*, **50**, No. 1, 39-45 (2014) (English translation).]

19. O. Madelung, U. Rössler, M. Schulz (eds.), *Zinc Sulfide (ZnS) Property: Energy Gap, Cubic Modification*, SpringerMaterials - The Landolt-Börnstein Database. Vol. 41B, Springer-Verlag, Berlin, Heidelberg (1999).

20. A. L. Stroyuk, A. I. Kryukov, S. Ya. Kuchmii, and V. D. Pokhodenko, *Teor. Éksp. Khim.*, **41**, No. 2, 67-87 (2005). [*Theor. Exp. Chem.*, **41**, No. 2, 67-91 (2005) (English translation).]

21. M. Godlewski and K. Swiatek, *Diluted Magnetic Semiconductors*, World Scientific, Singapore (1991), Ch. 16, pp. 621-642.